# Magnetic-closure domains and interpretation of spin-resolved electron spectroscopies

K. Starke,* K. Ertl, and V. Dose
*Max-Planck-Institut für Plasmaphysik–EURATOM Association, D-8046 Garching bei München, Federal Republic of Germany*
(Received 23 March 1992; revised manuscript received 1 June 1992)

In spin-resolved electron spectroscopies at surfaces that do not contain an easy axis of bulk magnetization, the detection of spin effects can be hindered by closure domains. This is demonstrated by combining the magneto-optical Kerr effect and spin-resolved inverse photoemission (IPE) using Ni(001) as an example. On a Ni(001) surface with high remanent magnetization, spin-resolved IPE reveals a spin splitting of (80±20) meV for transitions between bulk *sp* bands. The discrepancy in recent spectroscopic data regarding the splitting of Ni *sp* bands is explained by closure domains.

## I. INTRODUCTION

The main information in spin-resolved electron spectroscopies is contained in the spin asymmetry. In investigations of ferromagnetic surfaces, a quantitative interpretation of spin-resolved spectra requires knowledge of the surface magnetization. Momentum-resolved experiments using photoemission (PE) or inverse photoemission (IPE) afford remanently magnetized samples since the slow electrons with a kinetic energy of a few 10 eV are not compatible with the application of external fields. Yet, at remanence, the magnetic-surface domain structure can be very complex, depending on the orientation of the surface. In nickel the bulk crystalline anisotropy at room temperature favors spontaneous magnetization along the so-called *easy axes* ⟨111⟩. Thus the only low-index Ni surface containing easy axes is (110). At this surface bulk domains can reach the surface without generation of magnetic poles. By contrast, a very complex structure of small flux-closure domains has been found at Ni(001) (Refs. 1 and 2) and is also expected for Ni(111).[3]

In spin-resolved PE and IPE, the signal is usually averaged over a sample surface area of several $mm^2$ for sufficient intensity. Hence the *average surface magnetization* must be known for the quantitative determination of the spectral spin asymmetry. But at surfaces with closure domains, the average remanent magnetization is not known *a priori* and experiments on Ni(001) have revealed contradictory results: On Ni(001), Krause and Frey[2] observed *homogeneous* surface magnetization, whereas for the same surface on another sample a *vanishing average* magnetization was found.[4] This completely different behavior of the remanent surface magnetization is by no means understood. Yet it most probably provides the key to explaining a discrepancy in recent spectroscopical data. In a spin-resolved IPE investigation of an *sp*-band bulk transition on Ni(001) by Klebanoff *et al.*,[4] no positive identification of spin dependence was possible. But almost the same transition viewed from Ni(110) revealed a clearly resolved spin splitting of 140 meV.[5]

The purpose of the present work is to demonstrate the influence of flux-closure domains on the surface magnetization and hence on the size of spin effects in spin-resolved electron spectroscopies. As an example, we chose Ni(001). The surface magnetization is detected by two methods having very different information depths: The average magnetization in the top atomic surface layers is monitored by the spin asymmetry of an IPE transition into a *minority* 3*d* band. This surface magnetization is determined by the domains which reach the surface. Their magnetization is examined by a UHV-compatible magneto-optical Kerr effect (MOKE) setup.

This paper is structured as follows: Section II briefly summarizes results from earlier experiments and theoretical expectations regarding closure domains. After a description of experimental procedures in Sec. III, results on the temperature and field dependences of the Ni(001) magnetization will be presented and discussed in Sec. IV. In Sec. V it is demonstrated that the bulk *sp*-band IPE transition previously investigated by Klebanoff *et al.*[4] is clearly spin split when observed on the well-magnetized Ni(001) surface. The main conclusions are summarized in Sec. VI.

## II. DOMAIN MODELS

The domain structure of the Ni(001) surface was investigated in the 1960s by means of the Bitter technique. Rod-shaped single-crystalline Ni samples with the long axis parallel to ⟨110⟩ have a platelike structure of bulk domains.[1,2] They are magnetized along a ⟨111⟩ direction (see large domains in Fig. 1) and separated by (110)-71° walls normal to the long axis. At remanence the bulk-domain width was of the order of $\frac{1}{10}$ mm, whereas much finer powder patterns were found on the (001) surfaces. This demonstrated the existence of additional surface domains at Ni(001), but no information about their magnetization direction could be obtained.

A refined model of the domain structure at the Ni(001) surface was proposed by Krause and Frey[2] on the basis of a MOKE microscopy investigation. Figure 1 shows the model in a plane perpendicular to the (001) surface. In contrast to the bulk domains, the (gray-shaded) closure domains are not magnetized along an easy axis, but are *parallel* to the surface. Magnetic flux carried by the bulk domains does not penetrate the surface, but is directed to

 

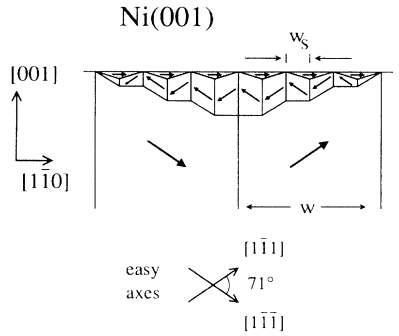


FIG. 1. Domain model for the remanently magnetized Ni(001) surface proposed by Krause and Frey (Ref. 2).

the neighboring bulk domains. As a result, the "stray" field energy contribution[6] to the total magnetic energy of the system is avoided at the expense of anisotropy energy. (Closure domains have nearly in-plane magnetization only in "magnetically soft" cubic crystals, where the anisotropy energy density is much smaller than the maximum field energy density.) The anisotropy energy contribution from the closure domains is kept small by having a small surface-domain width $w_s$ (see Fig. 1), which is two orders of magnitude smaller[7] than the bulk-domain width $w$; the connection between bulk and closure domains is achieved by an "echelon pattern" of branching domains.

The domain model in Fig. 1 only contains closure domains which are magnetized along the [1$\bar{1}$0] direction, i.e., *parallel* to the average bulk magnetization. Hence the average Ni(001) surface magnetization at remanence is equal to saturation and thus even larger than the magnetization of the basic domains projected onto the surface. But already in very small external fields ($\sim 1$ A cm$^{-1}$) Krause and Frey[2] observed a pattern of oppositely magnetized domains, i.e., average surface magnetization well below saturation.

From the point of view of domain theory,[3] the model for the remanent surface in Fig. 1 is surprising in two respects. First, in "thick" cubic crystals (larger than 1 $\mu$m in all dimensions), the magnetization direction of branching and closure domains is not restricted to one plane, so that complex "three-dimensional" structures with many different magnetization directions can be realized. The average surface magnetization of these structures is expected to be much smaller than saturation. Second, the two-dimensional model in Fig. 1 does not describe the state of minimum energy: According to a calculation by Hubert,[3] such a two-dimensional structure, when optimized with respect to the total energy, contains closure domains magnetized *parallel* and others magnetized *antiparallel* to the [1$\bar{1}$0] direction. Consequently, if a two-dimensional structure applies at all to Ni(001), the *average* surface magnetization is theoretically expected to be *below* saturation.

In contrast to the model in Fig. 1, Klebanoff *et al.*[4] found in a MOKE study that the *average* Ni(001) surface magnetization *vanishes* at remanence. The shape of their sample differed from the above one: It was cut as a square plate with edges parallel to ⟨100⟩ and was mounted on a horseshoe iron magnet. However, this radically different behavior of the Ni(001) surface magnetization is as yet unexplained.

## III. EXPERIMENTAL DETAILS

The Ni(001) surface magnetization is detected by MOKE and spin-resolved IPE. Owing to the very different information depth of the two methods, it is possible to compare the magnetization of the domains which reach the surface with the magnetization of the top atomic surface layers. The MOKE measurements were made *in situ* at an UHV chamber for spin-resolved IPE, which is described in detail elsewhere.[22,24]

The Ni(001) sample employed in the present study is shown in Fig. 2(a). The single crystal has the shape of a square picture frame with legs all parallel to a ⟨110⟩ axis. This closed-flux geometry makes magnetic stray fields from the sample minimal, which is important for high angular resolution in the IPE measurements. Furthermore, because of the ⟨110⟩ orientation of the sample legs, the bulk domains have the same shape[8] as shown in Fig. 1. The present results on the Ni(001) surface magnetization can thus be compared with the model. The (001) surface was polished to a mirror finish by using diamond paste and afterward annealed for several hours at 800 °C *in situ* in the UHV chamber. In order to avoid strong Ni deposition on the insulation ceramics (Ni-vapor pressure at 1200 °C, $\sim 1\times 10^{-3}$ Pa), the sample was kept at high temperatures for only a short time, i.e., $\frac{1}{2}$ h at 1000 °C and a few minutes at 1200 °C. For the self-supporting magnetizing coil wound around the upper leg

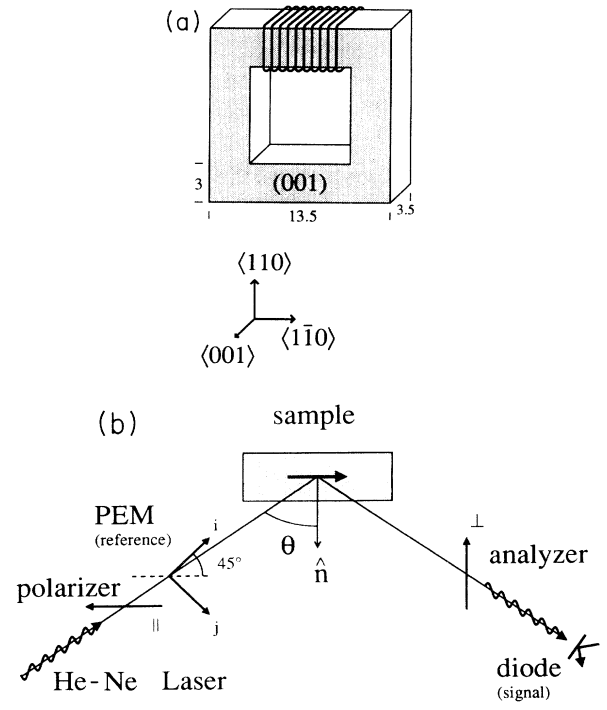


FIG. 2. (a) Single-crystalline nickel picture-frame sample. (b) Schematic of the MOKE setup.

[ten turns; see Fig. 2(a)], a noninsulated Ta wire was used to prevent electrostatic charging. The surface and bulk magnetization (see below) were measured at the lower leg. Apart from the demonstration of temperature hysteresis in Sec. IV D, remanent magnetization was achieved by short current pulses ($\sim$50 A, $\sim$1 ms) through the coil. Since the magnetization of nickel crystals is very sensitive to stress, massive electric contacts must be avoided. The sample was therefore heated by electron bombardment instead of a direct "Ohmic" heating. For preparation and characterization of the sample, conventional sputter facilities, low-energy electron diffraction (LEED), and Auger electron spectroscopy were employed.

The MOKE information depth is given by the light penetration depth of 100–200 Å. It is smaller than the domain-wall width (400 Å at room temperature[9]) which serves as a lower limit for the thickness of closure domains. MOKE is therefore only sensitive to the magnetization of domains which reach the surface. In particular, when closure domains are present at the surface, domains located underneath do not contribute to the MOKE signal. The laser beam was widened to a diameter of $\sim$1 mm, which is much larger than the mean domain width at the (001) surface (see Figs. 6, 7, and 1); thus, the spatial average of their magnetization is probed. The MOKE setup is shown schematically in Fig. 2(b). Modulation technique provides the high signal-to-background ratio necessary for detecting details of the complex room-temperature hysteresis loops (see Fig. 5).

The magnetization component parallel to the long axis of the leg ($[1\bar{1}0]$; see Fig. 2(a)) was measured by longitudinal MOKE. The center of the sample leg was irradiated at $\theta=23°$ relative to the surface normal. At off-normal incidence, it is possible, in principle, for a hypothetical magnetization component normal to the surface to contribute to the longitudinal MOKE signal.[10] By polar MOKE, using the same setup as in Fig. 2(b) with $\theta\sim0°$, it was found that the average normal magnetization vanishes at remanence. This finding is in agreement with the expectation of *in-plane* magnetization of the Ni closure domains (see Sec. II).

A known disadvantage of MOKE measurements is their sensitivity to thermal drift[11] of the whole setup, including the sample holder. Only *changes* of magnetization can therefore be reliably detected by this method. A hysteresis loop had to be completed on a time scale of a few 10 s. Yet, to demonstrate temperature hysteresis of the surface magnetization (in Sec. IV D), it was necessary to monitor the magnetization over a time span of 1.5 h, during which the sample cooled down from above $T_C=630$ K to almost room temperature. For this purpose the spin asymmetry of an IPE transition into the *minority d* band was employed. The large spin asymmetry of a direct *d*-band transition on Ni(100) has been used before as a magnetization detector at a fixed temperature.[12] The same *d* band, since it has almost no dispersion, can be observed as a density-of-states (DOS) contribution at Ni(001) (see Fig. 10). When the spin asymmetry is used as a monitor for the temperature dependence of the magnetization, the temperature-induced change of the Ni *d*-band exchange splitting must be considered as well as the temperature broadening of the Fermi edge. Both effects lead to a complex temperature dependence of the spin asymmetry near the Curie temperature, but have little influence further below.[13] It will be shown in Sec. IV D that below 500 K the spin asymmetry of the *d*-band transition on Ni(001) has the same temperature dependence as the average surface magnetization measured by MOKE. Below 500 K the spin asymmetry can thus be utilized to monitor changes of the average surface magnetization with temperature. At normal electron incidence, the transverse polarization of the electron beam is parallel to the long axis of the sample leg [see Fig. 2(a)] so that the same magnetization component as with longitudinal MOKE is probed. Owing to the much smaller IPE information[14] depth, the spin asymmetry is only sensitive to the magnetization of the outermost atomic layers. During IPE measurements, the heating filament was switched off to avoid stray magnetic fields.

The domain structure at the Ni(001) surface is observed by MOKE microscopy. Since no UHV-compatible MOKE microscopes are as yet available, the domain observation had to be performed *ex situ*. Before comparing the *ex situ* data with the MOKE data of the average surface magnetization obtained under UHV conditions, the latter data must be checked for possible influence of vacuum conditions. Neither extensive sputtering (vanishing LEED spots) nor absorption of several langmuirs of oxygen had an influence on the MOKE data. Obviously, the average magnetization of the domains at the Ni(001) surface is insensitive to the geometrical order and the chemical cleanliness of the outermost atomic layers. For MOKE microscopy at elevated temperatures, the crystal surface was viewed through the glass window of a small vacuum container (to avoid sample oxidation).

Bulk hysteresis curves of the sample were recorded *ex situ* by a 200-turn induction coil wound around the same sample leg at which the MOKE data have been obtained. The hysteresis loops were completed within 40 s, a time for which no smearing-out of the loop due to friction of domain-wall propagation[15] was observed. The voltage induced during the magnetization reversal was recorded as a function of the current through the magnetization coil and numerically integrated. The *simultaneously* measured MOKE hysteresis loop of the (001) surface was identical with that obtained *in situ*, so that surface and bulk magnetization in Figs. 4 and 5 may be directly compared.

## IV. TEMPERATURE AND FIELD DEPENDENCE OF THE SURFACE MAGNETIZATION

### A. Average magnetization

The temperature dependence of the average surface magnetization at remanence is shown in Fig. 3. As the sample cooled down, current pulses of opposite direction were sent through the magnetization coil (every few seconds) and the MOKE signal was recorded after each magnetization pulse. The difference of signals which correspond to two successive pulses is proportional to the

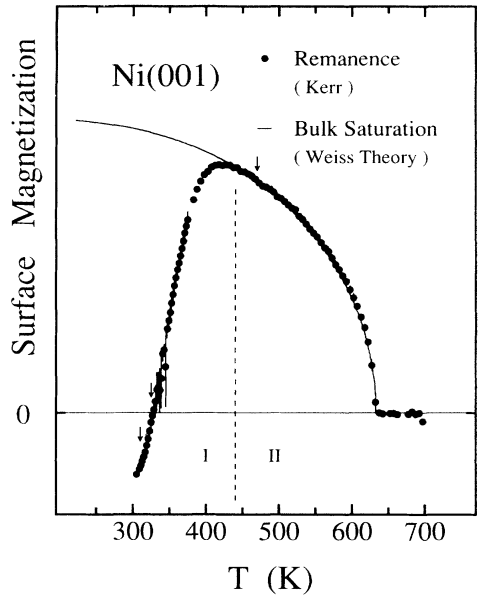


FIG. 3. Temperature dependence of the average remanent magnetization of the Ni(001) surface. Arrows indicate temperatures of the hysteresis loops in Fig. 5.

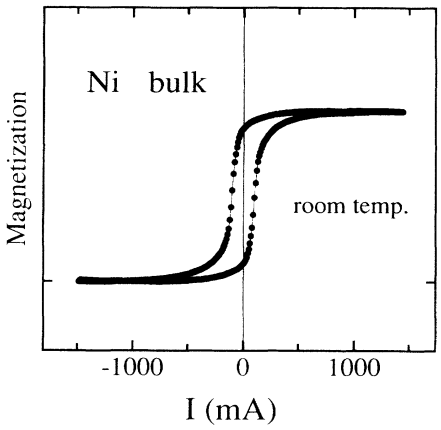


FIG. 4. Bulk hysteresis of the same sample leg at which surface magnetization is investigated.

remanent magnetization. (The measurement of magnetization differences provides insensitivity to long-term drift of the setup; see Sec. III.) Figure 3 comprises three single runs in temperature intervals of 5 K (above 380 K) and 2 K (below 380 K). The solid line describes the saturation magnetization according to the molecular-field theory of Weiss. Using spin $=\frac{1}{2}$ and $T_C=630$ K as parameters, it approximates the temperature dependence of Ni bulk saturation[16] sufficiently well for the intended comparison with the surface magnetization. The MOKE data were scaled by adjusting the ordinate value at 460 K to the theoretical curve.

Above 440 K no difference between average surface magnetization and bulk saturation can be observed. Below 440 K the surface magnetization drastically decreases with temperature and vanishes at 330 K. At room temperature it is even *antiparallel* to the average bulk magnetization. The remanent magnetization in Fig. 3 is a unique function of temperature: By heating the sample to *any* temperature (starting at room temperature), the same temperature dependence was obtained. In keeping with the completely different behavior of the magnetization at low and high temperature, we shall distinguish between temperature ranges I and II.

The magnetization in range I is only reduced at the surface, but not in the bulk. This is evident from the bulk hysteresis curve shown in Fig. 4. It is measured at the *same* sample leg at which the MOKE data were obtained. At room temperature the bulk has high remanent magnetization. It must therefore be concluded that the strong decrease of the remanent surface magnetization in range I is not due to an ill-magnetized bulk, but a consequence of domains at the surface.

In range II the surface magnetization is the same as for surfaces which have a simple domain structure without closure domains. This is possible if the easy axes are not $\langle 111 \rangle$, but parallel to the (001) plane. It has been observed[17] that the first anisotropy constant changes sign at high temperature, resulting in "switching" of the easy axes to $\langle 100 \rangle$. Yet, according to Darby and Isaac,[18] the sign change occurs above 470 K, where no switch of the easy axes is indicated in Fig. 3: Range II extends down to 440 K.

The key to interpreting the temperature dependence is given by the field dependence of the surface magnetization, shown in Fig. 5. The three temperatures are marked by arrows in Fig. 3. The hysteresis curves are

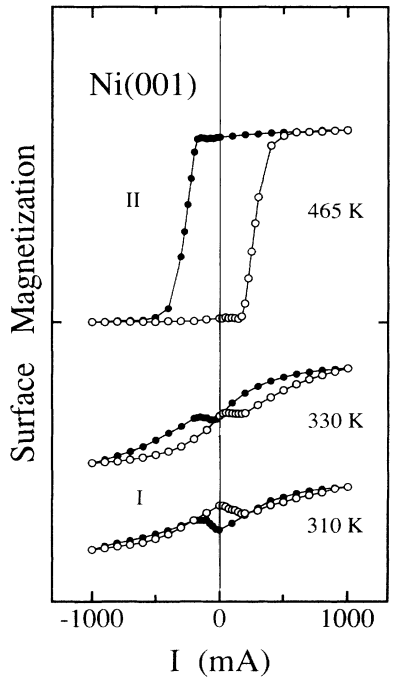


FIG. 5. Field dependence of the average Ni(001) surface magnetization in the temperature ranges of large (I) and negligible magnetic anisotropy (II). Note the finite (vanishing) slope of the magnetization at high currents in range I (II).

plotted versus the current through the magnetization coil. In Fig. 5, 1000 mA are equivalent to a field of 2.5 $A\,cm^{-1}$ on the assumption that the field is equal in all sample legs and homogeneous across their cross section. (The degree to which this assumption is valid depends on the domain structure and can be checked within the scope of the present experiment only for fields not smaller than 1.5 $A\,cm^{-1}$; see below. Therefore we prefer to use the current as coordinate.) The hysteresis loop at 465 K has a nearly rectangular shape characteristic of surfaces containing an easy axis where bulk domains reach the surface without closure domains. The loops have such a simple form in the whole range II. By contrast, they have almost collapsed near room temperature: At 330 K the branches touch at remanence, and at 310 K they cross. (The values of remanent magnetization are about the same as in Fig. 3, although much larger maximum fields were applied there.)

The hysteresis loop in range II contains an important feature. The magnetization reversal is not "vertical": Starting from remanence, the reversal begins at 200 mA, but it is necessary to increase the external field up to 600 mA in order to complete it. In general, the magnetization of large single crystals reverses in small external fields owing to the growth of oppositely magnetized domains, i.e., mainly by movement of 180° domain walls. In well-annealed Fe-Si picture-frame crystals with all surfaces containing an easy axis the nucleation of oppositely magnetized domains occurs by detachment of a 180° wall from a surface when the external field surmounts a "starting" field $H_s$.[15] If the field necessary for the subsequent movement of the wall is smaller than $H_s$, the magnetization of the crystal completely reverses at $H_s$ ("Barkhausen jump"). By contrast, the nonvertical flanks of the surface hysteresis in range II show that the growth of oppositely magnetized domains is hindered by friction of domain-wall motion.

The friction of wall motion is a consequence of imperfections in real crystals, which lead to locally varying internal stress and hence to a spatially dependent energy of domain walls.[16] Magnetization reversal of a crystal can only be completed if the external field is sufficiently large to allow walls between oppositely magnetized domains to pass the crystal imperfections. The upper loop in Fig. 5 reveals constant surface magnetization above 600 mA, thus indicating that the magnetization is completely reversed. Yet unique identification of a complete reversal is only possible by observing the surface-domain structure.

### B. Domain structure

The sign reversal of the average surface magnetization in Fig. 3 already shows that closure domains with a magnetization component *antiparallel* to the average bulk magnetization must exist at room temperature. The structure of the closure domains at room temperature is shown in Figs. 6(a) and 6(b); the *ex situ* MOKE microscopy images present domains of the same surface area ($250\times170$ $\mu m^2$). In Fig. 6(a) the light polarization is chosen such that a magnetic contrast is generated by differences of the component parallel to the $[1\bar{1}0]$ direction as in the above MOKE measurements of the average magnetization. The domains are ordered in strips perpendicular to this direction. They cannot be extinguished even in the highest external fields available ($\sim10$ $A\,cm^{-1}$), in agreement with the nonvanishing slope of the hysteresis loops in Fig. 5. The contour of the domains is fairly arbitrary, and their average size varies over the surface (compare the left and right halves of Fig. 6). At remanence light and dark strips have a width of about 40 $\mu m$.

For Fig. 6(b) the light polarization was rotated 90° so that the magnetic contrast *perpendicular* to the $[1\bar{1}0]$ direction becomes visible. It is much weaker than the contrast of the $[1\bar{1}0]$ magnetization component in Fig. 6(a). A weak contrast implies that the perpendicular component itself is small, since it must vanish on the average over many closure domains (avoidance of magnetic charges). Hence the closure domains are magnetized mainly *parallel* or *antiparallel* to the average bulk magnetization. The structure thus differs from the homogeneous magnetization observed by Krause and Frey.[2] However, there is no contradiction between their finding and the present results: At remanence the wall friction partly conserves the closure-domain structure present with nonvanishing fields (see below), for which also

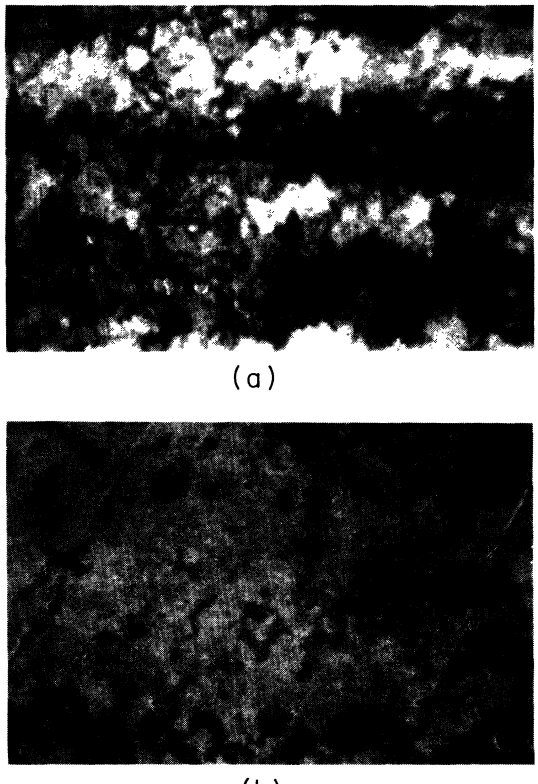


FIG. 6. MOKE microscopy images of the remanently magnetized Ni(001) surface at room temperature. The magnetic contrast is due to different magnetization components located in the surface: *a*, parallel to the axis of the sample leg; *b*, perpendicular. All images show the same surface area ($250\times170$ $\mu m^2$).

Krause and Frey report the existence of both parallel and antiparallel domains. (One should keep in mind that the model in Fig. 1 might not apply to thick crystals since it is only "two dimensional" and that it is *not* minimized with respect to the total energy; see Sec. II.)

The MOKE microscope pictures in Figs. 7(a)–7(c) were taken during magnetization reversal in range II along a hysteresis branch. As in Fig. 6(a), the contrast is due to the magnetization along $[1\bar{1}0]$. At $-1000$ mA [Fig. 7(a)], the contrast completely vanishes. When the field is reduced down to remanence, small randomly distributed domains emerge which occupy only a few percent of the surface area [Fig. 7(b)]. When the field is increased beyond $+200$ mA, larger domains of opposite magnetization suddenly appear which, in contrast to the small domains at remanence, are ordered in strips parallel to the $[1\bar{1}0]$ direction [Fig. 7(c)]. Upon further increase of the field, the opposite domains grow until the contrast again vanishes at $+600$ mA and above. These observations agree well with the range-II hysteresis curve of the average magnetization in Fig. 5.

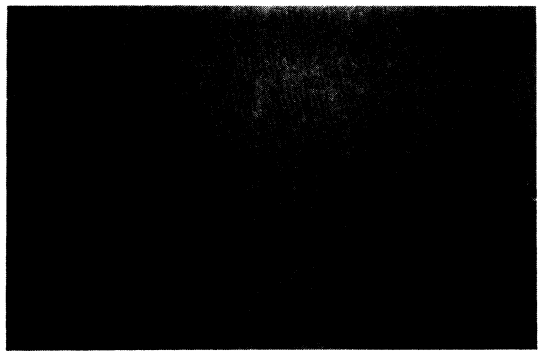

(a)

(b)

(c)

FIG. 7. MOKE microscopy images of Ni(001) surface domains obtained during magnetization reversal in the temperature range of negligible anisotropy ($T=490$ K). Currents through the magnetization coil: (a) $-1000$ mA, (b) 0 mA, and (c) $+260$ mA. All images show the same area ($250\times170\ \mu m^2$).

The vanishing contrast uniquely demonstrates that in temperature range II a current of 600 mA is indeed sufficient to achieve a *complete* reversal of the surface magnetization. From the fact that neither closure nor stress domains exist, we conclude that the *surface is magnetized in plane.* Furthermore, Fig. 4 shows that also the bulk magnetization is fully reversed at 600 mA. (Although measured at room temperature, the bulk magnetization is expected to be reversed at this current at higher temperatures as well since the nickel bulk coercitivity hardly changes in the temperature interval considered here.[16]) The external field is therefore approximately *homogeneous* across the sample leg at 600 mA (and above).

### C. Magnetic energies and interpretation

On the basis of this observation, we can estimate the contributions to the total magnetic energy in temperature range II. With equal fields assumed in all sample legs, the current of 600 mA is equivalent to a field $\mathbf{H}=1.5$ A cm$^{-1}$. In view of the homogeneity of the field, we need only consider energy densities. Relevant contributions to the total magnetic energy density $e_{\rm tot}$ are the magnetostatic energy $e_H=-\mathbf{J}\cdot\mathbf{H}$ ($\mathbf{J}$ is the magnetization), anisotropy energy $e_K$, and stress energy $e_\sigma$:

$$e_{\rm tot}=e_H+e_K+e_\sigma\ , \tag{1}$$

whereas stray field energy and wall energy can be neglected in the absence of closure domains. The applied field of 1.5 A cm$^{-1}$ is equivalent to $e_H\approx1000$ erg cm$^{-3}$. In the whole range II, the value of the first anisotropy constant $K$ is smaller than 1000 erg cm$^{-3}$,[17] which leads to an upper bound of $e_K\approx K/3\approx300$ erg cm$^{-3}$. Hence the crystal anisotropy is reduced to such an extent that the sample, if $e_\sigma$ is not too large (see below), can already be homogeneously magnetized by the small field of 1.5 A cm$^{-1}$. The magnetization is along $\mathbf{H}$, i.e., parallel to the leg, *independently* of the directions of easy magnetization. This estimate is consistent with the observation of vanishing magnetic contrast in Fig. 7(a) and constant magnetization above 600 mA in Fig. 5.

By means of Eq. (1), we can obtain an upper bound for the amount of crystal stress present at the (001) surface. At fields of 1.5 A cm$^{-1}$ (and above), crystal stress has no influence on the surface magnetization. Hence the stress energy density $e_\sigma\approx\frac{3}{2}\lambda\sigma$ (Ref. 6) must be smaller than the magnetostatic energy $e_H$, $\sigma$ and $\lambda$ denote the crystal stress and the (isotropic) magnetostriction constant, respectively. By equating the two energy densities, one obtains a stress density of $\sigma\leq200$ N cm$^{-2}$; it serves as an upper bound since $e_K$ is neglected here. The crystal

stress of the present sample is thus at least five times as small as other "well-annealed" Ni samples.[27] [In principle, crystal stress can be of internal as well as external origin. The internal stress strongly depends on the sample preparation and is nearly temperature independent.[16] External stress could be imposed by the clamps holding the sample. This possible influence was checked by *ex situ* MOKE hysteresis loops of the (110) surface: The loops recorded after removal of the clamps were identical to those obtained from the clamped crystal, so that a significant contribution of external stress can be excluded.]

When in range II the external field is reduced toward remanence, wall friction becomes important. It partly "conserves" the domain structure present with nonvanishing fields. Let us consider the case in which the easy axes are parallel to ⟨111⟩. A complex structure with closure domains then has a lower energy at remanence than the homogeneous magnetization parallel to the sample leg (direction of the former field). However, the closure-domain structure has a fine network of coupled domain walls. The structure will only be assumed in part since nucleation and growth of domains are hindered by wall friction. The temperature behavior of the remanent magnetization in Fig. 3 can thus be understood in the following way. At high temperatures, where the anisotropy is small, the sample leg is homogeneously magnetized parallel to its axis during the magnetization pulse. At remanence (when the pulse has terminated), a reconstruction of domains will occur only if the associated gain of anisotropy energy is sufficiently large to (partly) overcome the wall friction. Yet the anisotropy energy and hence any possible gain are too small in the whole range II. Only below 440 K (range I) can a structural reorganization of the domains take place since the hereby gained anisotropy energy suffices to surmount the wall friction. The temperature of transition between ranges I and II is therefore determined by wall friction; it is *not* identical with the "switching" temperature of the easy axes.

In any experiment in which remanence is prepared through a magnetization pulse, a domain structure of higher energy can be (partly) conserved by wall friction and a change in easy axes becomes apparent only at temperatures *below* the "switching" temperature. A "rather curious effect" was observed by Abraham and Hopster at a (110) surface of a Ni picture-frame crystal.[14] It had the same orientation as the sample used in the present work. If the switch of the easy axis (expected by Abraham and Hopster at ~370 K) were followed by a break-up into domains, the average surface magnetization should be reduced by 20%. Yet there was no indication of such a change in their spin polarization data. Since in their case remanent magnetization was also achieved by current pulses, the effect can be well explained by wall friction.

It is well known that the crystal stress depends on the preparation, i.e., temperature and duration of the annealing procedure. At surfaces the amount of stress is strongly influenced by polishing and the extent to which chemical etching is employed.[19] Thus the amount of crystal stress and defects may be widely different for different samples.

At surfaces with closure domains, the average magnetization is determined by the relative size of differently oriented domains (see Sec. II and Fig. 6). Since details of a surface-domain pattern are stress dependent,[20] we expect that at a surface with closure domains the average magnetization depends on the *individual* sample.

### D. Temperature hysteresis

The Ni(001) surface-domain structure at remanence greatly changes when going from high to low temperature. A reconstruction of the domains is accompanied by wall motion, for which the presence of friction has been identified above. The domain structure—such as in an external field—must therefore be expected not to change uniquely with temperature, but to show hysteresis.

Temperature hysteresis of a domain structure has already been observed by Schauer[21] on Ni(110). ac demagnetization of the sample at room temperature resulted in a regular structure of platelike domains separated by 71° walls. When the sample was heated without exposure to external fields, this structure remained unchanged up to the Curie temperature $T_C$. On surpassing $T_C$ and subsequent cooling (again avoiding external fields), a structure of randomly oriented small stress domains appeared below $T_C$. Again, these domains remained unchanged upon cooling down to room temperature. The regular domain pattern reappeared only upon idealization or further cooling to 220 K. Schauer expects temperature hysteresis for every Ni sample independently of the surface orientation, but up to now there have been no such investigations on surfaces with closure domains.

The temperature dependence of the average surface magnetization is shown in Figs. 8 and 9. As an indicator for the magnetization, we used the spin asymmetry of an IPE transition into a 3*d* band (see Fig. 10). Since the spin

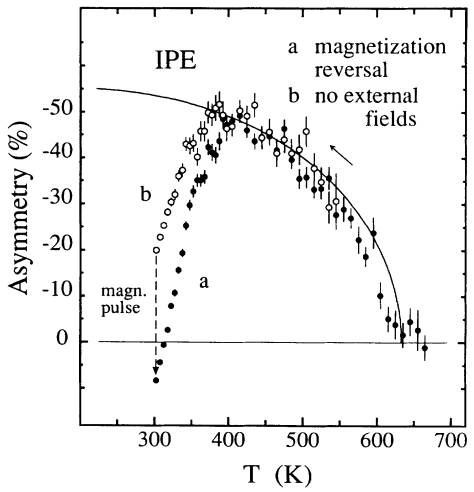


FIG. 8. Temperature dependence of the remanent surface magnetization monitored by the 3*d*-band asymmetry in IPE (see Fig. 10): (a) While cooling down the sample, magnetization is reversed at each data point. (b) The sample magnetized at 540 K cools down without external fields. A magnetization pulse changes the surface magnetization. The solid line indicates the theoretical saturation magnetization (see Fig. 3).

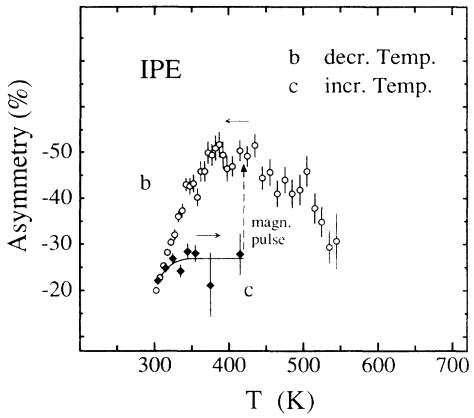


FIG. 9. Temperature hysteresis of the remanent surface magnetization (see text). The temperature cycle is indicated by small arrows.

asymmetry probes the magnetization of the uppermost atomic layers, it is sensitive to surface contamination and roughness on the atomic scale (unlike the magnetization probed by MOKE; see Sec. III). The high surface quality of our sample was checked by (i) the crystal-induced surface state at Ni(001) $\bar{X}$,[22] which decreased in intensity only by $\sim 10\%$ during a cooling-heating cycle ($\sim 2$ h) and (ii) the *d*-band asymmetry itself. For each curve *a*, *b*, and *c*, data from many single temperature cycles (with and without magnetization pulses) were accumulated to improve counting statistics. Data for curves *a* and *b* were recorded during the cooling-down phase of the sample. For curve *a* the sample magnetization was reversed by current pulses at each temperature so that two asymmetry curves were obtained; they only differed by sign and are represented by curve *a*. Below 500 K one finds the same temperature dependence of the magnetization as the MOKE data in Fig. 3. (As seen by MOKE with a focused laser beam [$\sim 0.2$ mm full width at half maximum (FWHM)], the magnetization is slightly enhanced at the edges of the sample leg in the high-anisotropy range. In this range curve *a* lies above the MOKE curve in Fig. 3 because the electron-beam cross section was larger than that of the laser beam.) When, by contrast, the sample is remanently magnetized at 540 K, i.e., at a temperature of negligible anisotropy, and subsequently cools down to room temperature without exposure to external fields, one obtains curve *b*. It cannot be distinguished from *a* in the low-anisotropy range. The magnetization reduction in *b* with respect to saturation (solid line in Figs. 8 and 9) occurs only below 380 K and is less steep than in case *a*. At room temperature the average magnetization is still about $\frac{1}{3}$ of the saturation and is oriented *parallel* to the average bulk magnetization. By application of a magnetization pulse, the surface magnetization changes irreversibly from *b* to *a*. In contrast to *a*, curve *b* is not a unique function of temperature. This is shown in Fig. 9: When the sample, after being remanently magnetized at 540 K and cooled down without external fields (curve *b*), is heated again, the magnetization deviates from *b* above 320 K and stays constant within counting statistics above 350 K (curve *c*). (In heating the sample, stray fields of the filament could not be avoided; yet, curve *c* is independent of the direction of the filament current.) Only above 440 K, i.e., at negligible anisotropy, was the surface magnetization affected by the stray fields of the filament. After completion of the cooling-heating cycle, during which the magnetization changes along curves *b*/*c*, a single magnetization pulse sufficed to yield irreversibly high magnetization, e.g., at 420 K (see dashed arrow in Fig. 9).

The remanent domain structure of Ni(001) thus shows pronounced temperature hysteresis, as expected. The change of magnetization without external fields (curve *b*) already occurs above 220 K, which was reported by Schauer.[21] This is plausible because of the much lower crystal stress (see above) of the sample used in the present work. The temperature hysteresis demonstrates that the surface magnetization depends on the history of *both* parameters: field and temperature. For the presently investigated Ni(001) surface, it even determines whether the average surface remanence is *parallel* or *antiparallel* to the surface-projected bulk magnetization.

## V. CONSEQUENCES FOR SPIN-RESOLVED SPECTROSCOPIES

Comparing the temperature dependence of the average surface magnetization (in Fig. 3) with the spin asymmetry (curve *a* in Fig. 8) shows that closure domains can hinder the detection of spin effects in spin-resolved electron spectroscopies. This important point will be further illustrated.

In the first spin-resolved IPE measurement of Ni(001) by Klebanoff *et al.*,[4] a surprisingly small spin asymmetry of $-10\%$ was obtained for the transition into the *minority* 3*d* band (at normal electron incidence). Furthermore, no spin splitting was identified for an intense *sp*-band transition. The finding was in accord with the expectation of the authors: "One would not expect a sizable spin dependence for a large bandwidth 4*sp* band."[4] However, almost the same transition showed a clearly resolved spin splitting of 140 meV, when viewed from the (110) surface.[5] It was this discrepancy which initiated our present study.

In the investigation by Klebanoff *et al.*,[4] the average remanent magnetization of the (001) surface was found to vanish at room temperature. In order to obtain a nonvanishing spin asymmetry for the *d*-band transition, an external field was applied. Yet this did not increase the surface magnetization beyond $\frac{1}{3}$ of saturation, since the applied field already led to a deflection of the incident electrons by 14°. This clearly shows that it is necessary to use *remanently* magnetized samples if high angular resolution is to be obtained in experiments using low-energy electrons.

In the present work, a high average Ni(001) surface magnetization was achieved without steady application of an external field; we employed the pronounced temperature hysteresis of the domain structure. The sample was remanently magnetized at 540 K and cooled down to 340 K within $\frac{1}{2}$ h of measurement time (curve *b* in Fig. 8). In

this temperature interval, the average $d$-band spin asymmetry was $-45\%$. Thus it was only reduced by $\frac{1}{10}$ as compared with a hypothetical asymmetry of the saturated surface ($-50\%$ at 400 K; see Fig. 8).

Figure 10 shows IPE spectra for normal electron incidence on Ni(001), spin-resolved spectra in the lower half and the spin-integrated spectrum along with the associated spin asymmetry above. The minority $3d$-band transition appears as the structure $B_1$ at 0.2 eV above the Fermi energy $E_F$. The asymmetry is much larger ($-45\%$) than in the previous measurement by Klebanoff *et al.*[4] and was used to monitor the surface magnetization. $B_1$ contains "density-of-states transitions" and a direct $\Delta_1$-$\Delta_5$ transition. The direct transition is weak since it occurs close to the $X$ point of the Brillouin zone; exactly at the $X$ point, it is dipole forbidden.[23] (The DOS contribution is experimentally identified by the small intensity decrease of $B_1$ upon disordering the surface.) The dipole-allowed $\Delta_1$-$\Delta_1$ transition into the $4sp$ band leads to the dominating peak $B_2$ at 1.4 eV above $E_F$. The spin-resolved spectra clearly demonstrate a nonvanishing splitting.

The spin-resolved spectra refer to a hypothetical polarization of the electron beam of 100%. The count rates $N\uparrow$ ($N_\downarrow$) expected in this case for electrons with spin parallel (antiparallel) to the average surface magnetization $\mathbf{J}$ are calculated from the count rates $n_{\uparrow,\downarrow}$ (raw data) obtained with the experimental polarization $P=33\%$ (Ref. 22) by using

$$N_{\uparrow,\downarrow}=\frac{n_\uparrow+n_\downarrow}{2}(1\pm A)\,, \tag{2}$$

with the spin asymmetry defined as

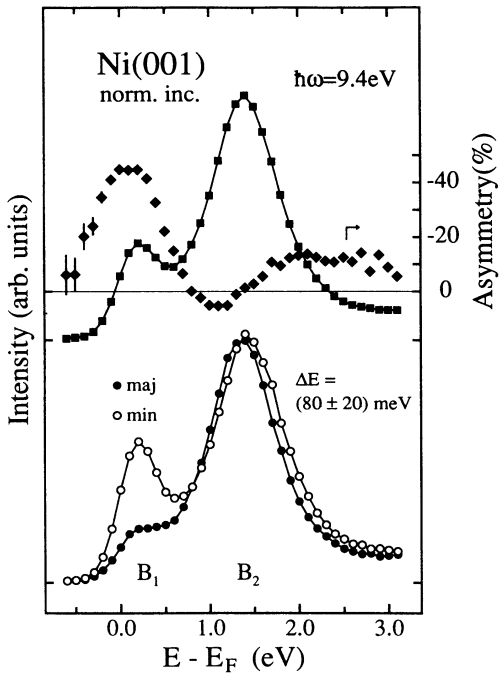


FIG. 10. Spin-resolved (bottom) and spin-integrated IPE spectra along with the associate spin asymmetry (top) at Ni(001), $\bar{\Gamma}$. $B_1$ and $B_2$ denote transitions into the minority $3d$ band and between $4sp$ bands, respectively.

$$A=\frac{n_\uparrow-n_\downarrow}{n_\uparrow+n_\downarrow}\frac{1}{P}\,. \tag{3}$$

The size of the spectral splitting is $80\pm20$ meV, as determined by least-squares fits of the spin-resolved spectra in Fig. 10. The error comprises the uncertainty of the electron-beam polarization[22] as well as a background contribution from $B_1$ not known *a priori*. A direct comparison of the spin-resolved spectra $N_{\uparrow,\downarrow}$ with theoretical band structures is only possible in the case of saturated samples, i.e., $\mathbf{J}=\mathbf{J}_s$. A reduced average surface magnetization $J<J_s$ leads to a smaller asymmetry $A$, which by virtue of Eq. (2) results in a smaller difference between the spectra $N_\uparrow$ and $N_\downarrow$. Since the FWHM of the lines ($\sim1$ eV) is much larger than their splitting, a reduced difference between $N_\uparrow$ and $N_\downarrow$ automatically leads to a reduced energy difference of the corresponding peaks. Thus the value of 80 meV is a *lower bound* with regard to the influence of closure domains. The most likely splitting can be estimated by using the temperature dependence of the $d$-band asymmetry (curve $b$ in Fig. 8). A hypothetically saturated surface over the whole temperature interval of measurement (540 down to 340 K) would result in an asymmetry about 1.1 times larger than that in Fig. 10. The higher asymmetry would correspond to a splitting of 90 meV.

The nonvanishing splitting directly demonstrates that either the initial, the final, or both bands of the transition are exchange split: Since both bands have nonvanishing slopes and the spectra are taken at a constant transition energy $\hbar\omega=9.4$ eV, the splitting of the transition depends not only on the exchange splittings of the initial ($\Delta E_{A,i}$) and final state ($\Delta E_{A,f}$), but also on the slope of both bands. Taking into account the symmetry of the bands, we expect the final state to be less split than the initial state. The latter lies close to the $X_1$ point (9.4 eV above $E_F$) of the bulk Brillouin zone, the final state close to $X_{4'}$.[23] At high-symmetry points, only wave functions of equal parity can mix. Because of the $p$-like symmetry of $X_{4'}$ (Shockley-inverted gap), the hybridization with "magnetic" $3d$ bands vanishes at the high-symmetry point and is small for the nearby final state. For the $X_1$ point, by contrast, band-structure calculations[25,26] reveal a large $s$-$d$ hybridization (30% of $3d$-like and more highly excited $d$-like wave functions), which gives rise to an exchange splitting of 200 meV. This considerable splitting has been demonstrated experimentally by spin-resolved target current spectroscopy (TCS).[22] According to the theoretical band structure by Noffke,[26] the initial-state splitting is expected to be $\Delta E_{A,i}=160$ meV and thus larger than the final-state splitting $\Delta E_{A,f}=80$ meV (both at $T=0$ K). For the splitting of the transition, a value between 80 and 160 meV must be expected since the initial and final bands have opposite slopes. The experimental value of 90 meV obtained at $\sim400$ K is in reasonable agreement with this expectation.

## VI. SUMMARY AND CONCLUSIONS

Closure domains can cause reduced or even vanishing average surface magnetization on Ni(001) and thus hinder the detection of spin effects in spin-resolved elec-

tron spectroscopies. At surfaces which do not contain an easy axis of bulk magnetization, the size and direction of the average surface magnetization are determined by details of the closure-domain pattern. We thus expect that "the" magnetization of such surfaces depends on the crystal stress of the individual sample, i.e., that it varies from one sample to another. Hence, for a quantitative interpretation of spin-resolved electron spectra, a concomitant investigation of the temperature and field dependence of the surface magnetization is mandatory for each individual sample.

## ACKNOWLEDGMENTS

We benefited greatly from the experimental and theoretical experience of M. Donath concerning IPE and surface magnetism. Valuable discussions with A. Hubert regarding the domain theory are gratefully acknowledged. The MOKE microscopy images shown in Sec. IV B were obtained at the Institut für Werkstoffwissenschaften in Erlangen, Germany, by R. Schäfer, to whom we express our thanks.

---

*Present address: Institut für Experimentalphysik, Freie Universität Berlin, Arnimallee 14, 1000 Berlin 30.

[1]H. Spreen, Phys. Status Solidi **24**, 413 (1967).

[2]D. Krause and H. Frey, Z. Phys. **224**, 257 (1969).

[3]A. Hubert, *Magnetic Domains* (Springer, Berlin, in press).

[4]L. E. Klebanoff, R. K. Jones, D. T. Pierce, and R. J. Celotta, Phys. Rev. B **36**, 7849 (1987).

[5]M. Donath, V. Dose, K. Ertl, and U. Kolac, Phys. Rev. B **41**, 5509 (1990).

[6]C. Kittel, Rev. Mod. Phys. **21**, 541 (1949).

[7]D. H. Martin, Proc. Phys. Soc. B **70**, 77 (1957).

[8]M. Donath, G. Schönhense, K. Ertl, and V. Dose, Appl. Phys. A **50**, 49 (1990).

[9]The thickness of Bloch walls in Ni is estimated by using $\sqrt{A/K}$ with the spin-coupling stiffness $A=8\times10^{-7}$ erg cm$^{-1}$ and the first anisotropy constant at room temperature, $K=5\times10^{4}$ erg cm$^{-3}$.

[10]J. Kranz and A. Hubert, Z. Angew. Phys. **15**, 220 (1963).

[11]K. Boockmann, diploma thesis, Universität Erlangen, 1989.

[12]M. Donath and V. Dose, Europhys. Lett. **9**, 821 (1989).

[13]The spin-asymmetry data of Ref. 12 at a fixed energy *above* the Fermi energy (e.g., +0.15 eV) show roughly the same temperature dependence as the bulk-saturation magnetization.

[14]D. L. Abraham and H. Hopster, Phys. Rev. Lett. **58**, 1352 (1987).

[15]G. Hellmiss, Wiss. Ber. AEG-Telefunken **43**, 77 (1970).

[16]E. Kneller, *Ferromagnetismus* (Springer, Berlin, 1962).

[17]G. Aubert, J. Appl. Phys. **39**, 504 (1968).

[18]M. I. Darby and E. D. Isaac, IEEE Trans. Magn. **MAG-10**, 259 (1974).

[19]W. Kranert and H. Raether, Ann. Phys. (Leipzig) 5, **43**, 520 (1943).

[20]W. Stephan, Ann. Phys. (Leipzig) 6, **15**, 337 (1955).

[21]A. Schauer, Z. Angew. Phys. **16**, 90 (1963).

[22]K. Starke, K. Ertl, and V. Dose, Phys. Rev. B **45**, 6154 (1992).

[23]A. Goldmann, M. Donath, W. Altmann, and V. Dose, Phys. Rev. B **32**, 837 (1985).

[24]U. Kolac, M. Donath, K. Ertl, H. Liebl, and V. Dose, Rev. Sci. Instrum. **59**, 1933 (1988).

[25]H. Eckardt and L. Fritsche, J. Phys. F **17**, 925 (1987).

[26]J. Noffke (private communication).

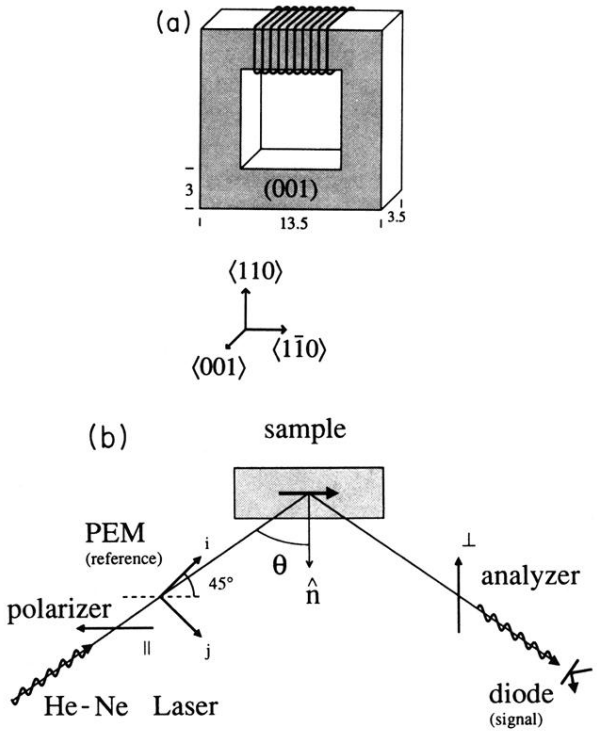


**FIG. 2.** (a) Single-crystalline nickel picture-frame sample. (b) Schematic of the MOKE setup.

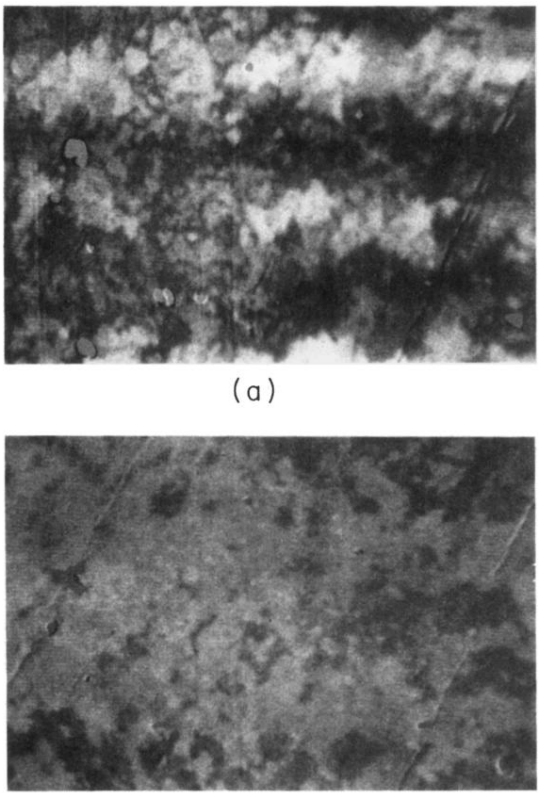


FIG. 6. MOKE microscopy images of the remanently magnetized Ni(001) surface at room temperature. The magnetic contrast is due to different magnetization components located in the surface: *a*, parallel to the axis of the sample leg; *b*, perpendicular. All images show the same surface area ($250 \times 170\ \mu m^2$).

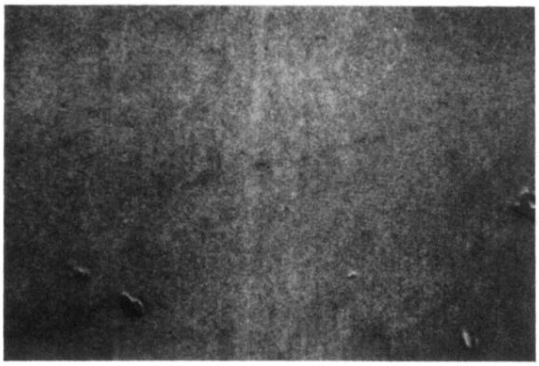

(a)

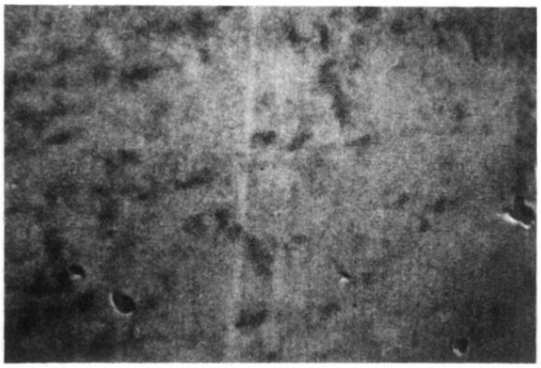

(b)

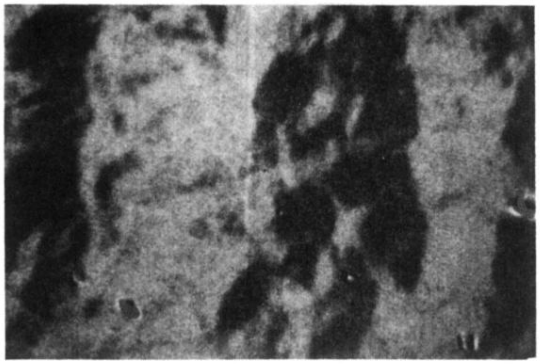

(c)

FIG. 7. MOKE microscopy images of Ni(001) surface domains obtained during magnetization reversal in the temperature range of negligible anisotropy ($T=490$ K). Currents through the magnetization coil: (a) $-1000$ mA, (b) 0 mA, and (c) $+260$ mA. All images show the same area ($250\times170\ \mu m^2$).